Eur. Phys. J. D (2020) 74: 125
https://doi.org/10.1140/epjd/e2020-10142-4

THE EUROPEAN PHYSICAL JOURNAL D

Regular Article

The role of the Debye screening of circular Rydberg states of hydrogenic systems in collinear electric and magnetic fields of arbitrary strengths

Nikolay Kryukov[1] and Eugene Oks[2,a]

[1] Universidad Nacional Autónoma de México, Av. Universidad 3000, col. Ciudad Universitaria, del. Coyoacán, México, DF 04510, México
[2] Physics Department, 380 Duncan Drive, Auburn University, Auburn, AL 36849, USA

Received 8 March 2020 / Received in final form 21 April 2020
Published online 18 June 2020

Abstract. We consider classical circular Rydberg states of a hydrogenic atom/ion under collinear electric and magnetic fields of arbitrary strengths, the entire system being immersed into a plasma with the Debye screening. In this way we add a "new dimension" to the results of the previous paper of one of us, where the screening was not taken into account. We show in detail how the screening decreases the value of the critical electric field required for the ionization at different values of the magnetic field. Our results should have a fundamental importance because hydrogenic atoms/ions under external fields remain a test-bench for atomic physics. Also our results could motivate experiments on the magnetic control of the "continuum lowering" in cold Rydberg plasmas, this being of practical importance.

1 Introduction

In paper [1] there was a study of a hydrogen-like system with the stationary nucleus of charge Z at the origin subjected to collinear electric ($\mathbf{F}$) and magnetic ($\mathbf{B}$) fields, the z-axis being chosen along the direction of $\mathbf{F}$ ($F_z > 0$). The Circular Rydberg States (CRS) of the electron were considered: the orbit, whose plane is perpendicular to Oz, has radius ρ and its center is on Oz at some point z.

In paper [1] the author derived analytical expressions for the energy E of classical CRS of hydrogenlike systems in collinear electric ($\mathbf{F}$) and magnetic ($\mathbf{B}$) fields of arbitrary strengths. He also offered formulas for the dependence of the classical ionization threshold $F_c(B)$ and of the energy at this threshold $E_c(B)$ valid for the magnetic field B of an arbitrary strength. In addition, for two important particular cases – classical CRS in a magnetic field only and classical CRS in an electric field only – some new results were presented in paper [1] as well[1].

In the present study, the same configuration as in paper [1] is considered to be submerged into a plasma with the Debye screening. We show in detail how the Debye screening decreases the critical value of the electric field required for ionization at various values of the magnetic field. Both the electric and magnetic fields are considered to be of arbitrary strengths, as in paper [1].

2 Results

For a hydrogen atom or a hydrogen-like ion, the allowance for the Debye screening is effected by replacing the Coulomb potential with the screened Coulomb potential:

$$\frac{Z}{r} \to \frac{Z}{r} e^{-r/a} \tag{1}$$

where a is the parameter of the plasma called the screening length (atomic units are used in this study: $\hbar = e = m_e = 1$). In the cylindrical coordinates, the classical Hamiltonian from paper [1] can be rewritten in the form

$$H(\rho, z) = \frac{L^2}{2\rho^2} - \frac{Z}{\sqrt{\rho^2 + z^2}} e^{-\sqrt{\rho^2+z^2}/a} + Fz + \Omega L + \frac{\Omega^2 \rho^2}{2} \tag{2}$$

where $\Omega = B/(2c)$. Here $L = \text{const}$, it is the z-component of the angular momentum, and Ω is the Larmor frequency.

[a] e-mail: goks@physics.auburn.edu

[1] There have been lots of theoretical and experimental studies of CRS (see, e.g., papers [2–5] and references therein) because: 1) their properties facilitated works on inhibited spontaneous emission and cold Rydberg gases (see, e.g., papers [6–8]; 2) classical CRS are counterparts of quantal coherent states; 3) in the quantal method using the expansion in terms of the inverse value of the principal quantum number, classical CRS are the primary term (see, e.g. paper [8] and references therein).

With the scaled quantities

$$v = \frac{Z}{L^2}\rho, w = \frac{Z}{L^2}z, f = \frac{L^4}{Z^3}F, \omega = \frac{L^3}{Z^2}\Omega, h = \frac{L^2}{Z^2}H,$$
$$\varepsilon = \frac{L^2}{Z^2}E, \lambda = \frac{L^2}{Za} \tag{3}$$

the expression for the Hamiltonian takes the following form:

$$h = \frac{1}{2v^2} - \frac{1}{\sqrt{w^2+v^2}}e^{-\lambda\sqrt{w^2+v^2}} + fw + \omega + \frac{\omega^2 v^2}{2}. \tag{4}$$

The conditions for the dynamic equilibrium are

$$\frac{\partial h}{\partial w} = 0, \frac{\partial h}{\partial v} = 0. \tag{5}$$

From the first equation in (5) we obtain

$$f = -\frac{w\left(1+\lambda\sqrt{w^2+v^2}\right)e^{-\lambda\sqrt{w^2+v^2}}}{\left(w^2+v^2\right)^{3/2}} \tag{6}$$

from where we see that for $f > 0$, $w < 0$. From the second equation in (5) we obtain

$$\frac{\left(1+\lambda\sqrt{w^2+v^2}\right)e^{-\lambda\sqrt{w^2+v^2}}}{\left(w^2+v^2\right)^{3/2}} + \omega^2 = \frac{1}{v^4}. \tag{7}$$

From (6) and (7) a more simple relation can be derived:

$$\omega^2 - \frac{f}{w} = \frac{1}{v^4} \tag{8}$$

which is independent of λ. From here we obtain the value $w(v, f, \omega)$ corresponding to the equilibrium:

$$w(v, f, \omega) = \frac{f}{\omega^2 - \frac{1}{v^4}}. \tag{9}$$

Then we substitute this equilibrium value of w into (6) and obtain an implicit equation for $f(v, \omega)$, which can be presented in the following form:

$$e^{-\lambda k}(1+\lambda k) = -\left(\omega^2 - \frac{1}{v^4}\right)k^3 \tag{10}$$

where

$$k = \sqrt{v^2 + \left(\frac{f}{\omega^2 - \frac{1}{v^4}}\right)^2}. \tag{11}$$

We numerically solve this equation and obtain the value $f(v, \omega, \lambda)$. Then we substitute this value into w in (9), getting $w(v, \omega, \lambda)$ and then substitute the resulting values of f and w into (4), obtaining the value of energy $\varepsilon(v, \omega, \lambda)$ corresponding to the equilibrium. Thus, we obtain the parametric dependence $\varepsilon(f)$ with the parameter v for the given values of ω and λ.

Figures 1 and 2 show the dependence $\varepsilon(f)$ at $\lambda = 0.3$ for $\omega = 1$ and $\omega = -1$.

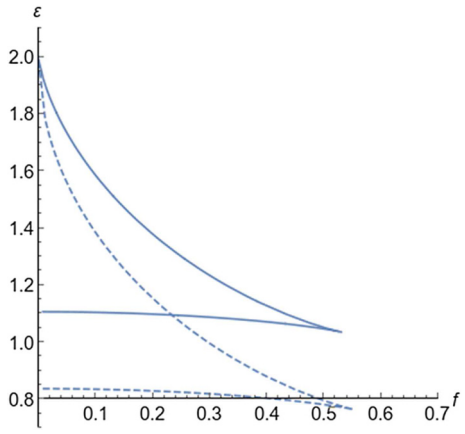

Fig. 1. The plot of the parametric dependence $\varepsilon(f)$ at $\lambda = 0.3$ for $\omega = 1$ (solid curves) compared to the same plot at $\lambda = 0$ (dashed curves).

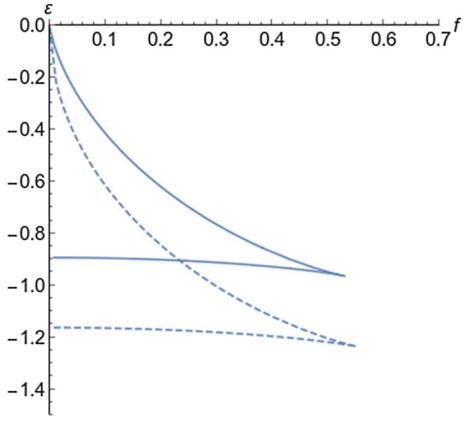

Fig. 2. The plot of the parametric dependence $\varepsilon(f)$ at $\lambda = 0.3$ for $\omega = -1$ (solid curves) compared to the same plot at $\lambda = 0$ (dashed curves).

The plots obtained for $\lambda = 0$ coincide with the corresponding plots in [1]. From the plots it is seen that the screening decreases the critical value of f required for ionization, because the screening lowers the continuum. To observe this effect more clearly, we made the similar plot, shown in Figure 3, for the case of $\omega = 0$ to remove the stabilization effect of the magnetic field.

We can see that the screening decreases the critical value of the electric field by a greater value in the case of $\omega = 0$.

Physically, the presence of two branches in each of the plots (solid or dashed) within Figures 1–3 has the following explanation. For each value of $f < f_c$, where f_c is the critical value beyond which there are no allowed values of the scaled energy ε, there are two values of the scaled equilibrium radius v of the orbit of the bound electron – as explained in paper [1] (see, especially Fig. 3 from paper [1]). One of the values corresponds to the lower energy branch, another – to the upper energy branch. According to paper [1], the lower energy branch corresponds to the stable motion of the bound electron, while the upper energy branch corresponds to the unstable motion of the

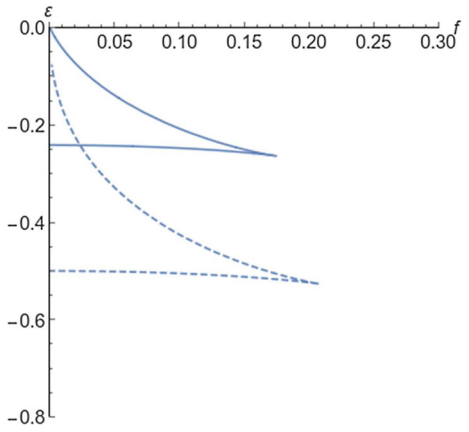

Fig. 3. The plot of the parametric dependence $\varepsilon(f)$ at $\lambda = 0.3$ for $\omega = 0$ (solid curves) compared to the same plot at $\lambda = 0$ (dashed curves).

bound electron. This means that the critical scaled field f_c, where the two energy terms cross, is the classical ionization threshold: at $f = f_c$, the system can switch from the stable motion to the unstable motion and to "slide" along the upper energy branch, so that the bound electron would end up in the continuum.

Next, we follow the procedure given in [1] to find the dependence of the critical value of f, f_c, on the scaled magnetic field ω. We can use either $\partial\varepsilon/\partial v = 0$ or $\partial f/\partial v = 0$ to find the scaled radius of the orbit corresponding to f_c; we use the first equation here, which yields

$$\frac{4}{v^5}\left(k^2 - v^2\right) = \left(\omega^2 - \frac{1}{v^4}\right)\left(v - k\frac{dk}{dv}|_c\right) \qquad (12)$$

where k is the solution of (10), and $(dk/dv)|_c$ can be found by differentiating (10) with respect to v:

$$\frac{dk}{dv}|_c = -\frac{4k^3}{v^5\left(\lambda e^{-\lambda k} - \lambda k\left(1+\lambda k\right) + 3k^2\left(\omega^2 - \frac{1}{v^4}\right)\right)}. \qquad (13)$$

Substituting (13) into (12) with k being the numerical solution of (10), we solve the resulting equation numerically for v to obtain the value $v_c(\omega, \lambda)$ corresponding to the ionization threshold. Substituting it further into the expression for the electric field $f(v, \omega, \lambda)$, we obtain the dependence $f_c(\omega, \lambda)$ of the critical electric field on the scaled magnetic field ω for a given value of the screening parameter λ.

Figure 4 shows the dependence of the critical electric field f_c on the scaled magnetic field ω for the values of $\lambda = 0$, 0.4 and 0.6. It is seen that the screening decreases the value of the critical electric field.

We also made the plot of $|\omega|(f_c)$, shown below.

The plot in Figure 4, as well as our corresponding calculations, can be used for finding the critical electric field for the ionization at different values of the magnetic field and of the screening parameter. The plot in Figure 5, as well as our corresponding calculations, can be used for finding the magnetic field at different values of the critical electric field for the ionization and of the screening parameter.

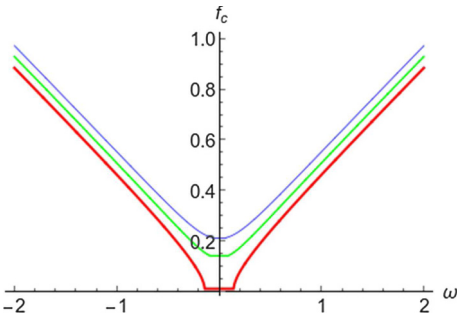

Fig. 4. The plot of the dependence $f_c(\omega)$ at $\lambda = 0$ (blue, thin top curve), $\lambda = 0.4$ (green, thicker middle curve) and $\lambda = 0.6$ (red, thick bottom curve).

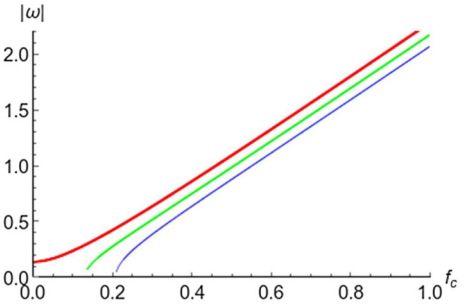

Fig. 5. The plot of the dependence $|\omega|(f_c)$ at $\lambda = 0$ (blue, thin bottom curve), $\lambda = 0.4$ (green, thicker middle curve) and $\lambda = 0.6$ (red, thick top curve).

For example, let us consider laser-produced plasmas emitting hydrogenic spectral lines that exhibit Langmuir-wave-caused dips (L-dips) in the profiles – such as, e.g., in experiments [10,11]. The L-dips arise from the resonance coupling of the Langmuir waves with a quasistatic electric field in plasmas; the coupling is facilitated by the radiation hydrogenic atom or ion – see, e.g., papers [2,13,14]. The L-dip phenomenon allows, in particular, to accurately measure both the electron density N_e and the quasistatic electric field F involved in the resonance. There were dozens and dozens of experiments by various groups around the world at different plasma machines, where such measurements were performed – see, e.g., books and reviews [15–18] and references therein.

Specifically, at laser-plasma experiments with the laser intensity $I \gg 10^{18}\,\mathrm{W/cm^2}$ (such as, e.g., the experiments [10,11]), GigaGauss (GG) and even multi-GG magnetic fields are expected to be developed during relativistic laser-plasma interactions: these fields should be localized at the surface of the relativistic critical density – see, e.g., review [19] and references therein. The ultra-strong magnetic field expected to arise in such experiments (the experiments exhibiting the L-dips) can be estimated using the results of our paper as follows.

From the experiment one would know the nuclear charge of the radiating ion Z and the principal quantum number n of the last observable Ly line. From the L-dips one would determine the electron density N_e and the characteristic value of the quasistatic electric field F (responsible for the L-dips). This value of F can be substituted in the

formulas from our paper as the critical electric field F_c. The temperature T can be estimated from the shape of the experimental spectral line profiles. Then one can calculate the screening parameter a (the Debye radius) and its scaled counterpart $\lambda \sim n^2/(Za)$. Next, one can estimate $f_c \sim F_c n^4/Z^3$. Then from our theoretical results for $\omega(f_c, \lambda)$, one can estimate ω. Next, one can estimate $\Omega(\text{a.u.}) \sim Z^2\omega(f_c, \lambda)/n^3$ and $\Omega(\text{s}^{-1}) = 4.13 \times 10^{16}\Omega(\text{a.u.})$, from where the estimate of the magnetic field can be obtained as $B = 2m_e c\,\Omega(\text{s}^{-1})/e$.

3 Conclusions

We considered classical CRS of a hydrogenic atom/ion under collinear electric and magnetic fields of arbitrary strengths, the entire system being immersed into a plasma with the Debye screening. By doing so, we added a "new dimension" to the results of paper [1], where the screening was not taken into account. We showed in detail how the screening decreases the value of the critical electric field required for the ionization at different values of the magnetic field[2].

Our results can be used for finding the critical electric field for the ionization at different values of the magnetic field and of the screening parameter. Alternatively, they can be used for finding the magnetic field at different values of the critical electric field for the ionization and of the screening parameter.

Our results should have a fundamental importance because hydrogenic atoms/ions under external fields remain a test-bench for atomic physics. As for the practical importance, it should be due to the fact that the results could motivate experiments on the magnetic control of the "Continuum Lowering" (CL) in cold Rydberg plasmas. The CL strongly influences radiative properties of plasmas (see, e.g. books/reviews [23–27] and references therein)[3].

Author contribution statement

Both authors contributed equally to this paper.

[2] A sufficiently strong magnetic field can lift energy terms into the continuum, as noted in paper [2]. These circular Rydberg states above the ionization threshold are classical molecular counterparts of the quantal atomic quasi-Landau levels (or resonances) discovered experimentally by Garton and Tomkins [21] (see, e.g., book [22] for theoretical references on atomic quasi-Landau resonances).

[3] Calculations of CL evolved from ion sphere models to dicenter models of the plasma state [25,28–33]. One of such theories - a percolation theory [3,25] - calculated CL defined as an absolute value of energy at which an electron becomes bound to a macroscopic portion of plasma ions (a quasi-ionization). In 2001 one of us derived analytically the value of CL in the ionization channel which was disregarded in the percolation theory: a quasimolecule, consisting of the two ion centers plus an electron, can get ionized in a true sense of this word before the electron would be shared by more than two ions [34].

References

1. E. Oks, Eur. Phys. J. D **28**, 171 (2004)
2. E. Lee, D. Farrelly, T. Uzer, Opt. Express **1**, 221 (1997)
3. T.C. Germann, D.R. Herschbach, M. Dunn, D.K. Watson, Phys. Rev. Lett. **74**, 658 (1995)
4. C.H. Cheng, C.Y. Lee, T.F. Gallagher, Phys. Rev. Lett. **73**, 3078 (1994)
5. L. Chen, M. Cheret, F. Roussel, G. Spiess, J. Phys. B **26**, L437 (1993)
6. S.K. Dutta, D. Feldbaum, A. Walz-Flannigan, J.R. Guest, G. Raithel, Phys. Rev. Lett. **86**, 3993 (2001)
7. R.G. Hulet, E.S. Hilfer, D. Kleppner, Phys. Rev. Lett. **55**, 2137 (1985)
8. K.B. MacAdam, E. Horsdal-Petersen, J. Phys. B **36**, R167 (2003)
9. V.M. Vainberg, V.S. Popov, A.V. Sergeev, Sov. Phys. JETP **71**, 470 (1990)
10. E. Oks, E. Dalimier, A.Ya. Faenov, P. Angelo, S.A. Pikuz, E. Tubman, N.M.H. Butler, R.J. Dance, T.A. Pikuz, I.Yu. Skobelev, M.A. Alkhimova, N. Booth, J. Green, C. Gregory, A. Andreev, A. Zhidkov, R. Kodama, P. McKenna, N. Woolsey, Opt. Express **25**, 1958 (2017)
11. E. Oks, E. Dalimier, A.Ya. Faenov, P. Angelo, S.A. Pikuz, T.A. Pikuz, I.Yu. Skobelev, S.N. Ryazanzev, P. Durey, L. Doehl, D. Farley, C.D. Baird, K.L. Lancaster, C.D. Murphy, N. Booth, C. Spindloe, P. McKenna, N. Neumann, M. Roth, R. Kodama, N. Woolsey, J. Phys. B: At. Mol. Opt. Phys. **50**, 245006 (2017)
12. A.I. Zhuzhunashvili, E. Oks, Sov. Phys. JETP **46**, 1122 (1977)
13. V.P. Gavrilenko, E.A. Oks, Sov. Phys. JETP **53**, 1122 (1981)
14. V.P. Gavrilenko, E.A. Oks, Sov. J. Plasma Phys. **13**, 22 (1987)
15. E. Oks, in *Plasma Spectroscopy: The Influence of Microwave and Laser Fields, Springer Series on Atoms and Plasmas* (Springer, Berlin, 1995), Vol. 9
16. E. Oks, in *Diagnostics of Laboratory and Astrophysical Plasmas Using Spectral Lineshapes of One-, Two-, and Three-Electron Systems* (World Scientific, Singapore, 2017)
17. E. Dalimier, E. Oks, O. Renner, Atoms **2**, 178 (2014)
18. E. Oks, E. Dalimier, A. Faenov, O. Renner, J. Phys. Conf. Ser. **548**, 012030 (2014)
19. V.S. Belyaev, V.P. Krainov, V.S. Lisitsa, A.P. Matafonov, Phys. Uspekhi **51**, 793 (2008)
20. M.R. Flannery, E. Oks, Phys. Rev. A **73**, 013405 (2006)
21. W.R.S. Garton, F.S. Tomkins, Astrophys. J. **158**, 839 (1969)
22. M. Brack, R.K. Bhaduri, in *Semiclassical Physics* (Addison-Wesley, Reading, Massachusetts, 1997), Sect. 1.4.2
23. R.P. Drake, in *High-Energy-Density-Physics: Fundamentals, Inertial Fusion, and Experimental Astrophysics* (Springer, Berlin, 2006), Sect. 3.2.2
24. S. Atzeni, J. Meyer-ter-Vehn, in *The Physics of Inertial Fusion: Beam Plasma Interaction, Hydrodynamics, Hot Dense Matter* (Oxford Univ. Press, New York, 2004), Sect. 10.1.4
25. D. Salzmann, in *Atomic Physics in Hot Plasmas* (Oxford University Press, Oxford, 1998), Chap. 2, 3
26. M.S. Murillo, J.C. Weisheit, Phys. Rep. **302**, 1 (1998)

27. H.R. Griem, in *Principles of Plasma Spectroscopy* (Cambridge University Press, Cambridge, 1997), Sects. 5.5, 7.3
28. J. Stein, I.B. Goldberg, D. Shalitin, D. Salzmann, Phys. Rev. A **39**, 2078 (1989)
29. D. Salzmann, J. Stein, I.B. Goldberg, R.H. Pratt, Phys. Rev. A **44**, 1270 (1991)
30. J. Stein, D. Salzmann, Phys. Rev. A **45**, 3943 (1992)
31. P. Malnoult, B. D'Etat, H. Nguen, Phys. Rev. A **40**, 1983 (1989)
32. Y. Furutani, K. Ohashi, M. Shimizu, A. Fukuyama, J. Phys. Soc. Jpn. **62**, 3413 (1993)
33. P. Sauvan, E. Leboucher-Dalimier, P. Angelo, H. Derfoul, T. Ceccotti, A. Poquerusse, A. Calisti, B. Talin, J. Quant. Spectrosc. Radiat. Transfer **65**, 511 (2000)
34. E. Oks, Phys. Rev. E **63**, 057401 (2001)